

IEICE **TRANSACTIONS**

on Electronics

DOI:10.1587/transele.2024MMP0003

Publicized:2024/06/11

**This advance publication article will be replaced by
the finalized version after proofreading.**

A PUBLICATION OF THE ELECTRONICS SOCIETY



The Institute of Electronics, Information and Communication Engineers

Kikai-Shinko-Kaikan Bldg., 5-8, Shibakoen 3chome, Minato-ku, TOKYO, 105-0011 JAPAN

Double Step Technique for Accurate Microwave High Attenuation Measurements

Anton WIDARTA, *non-member*

SUMMARY A double step attenuation measurement technique using a non-isolating gauge block attenuator (GBA) has been proposed for accurate measurements of radio frequency and microwave high attenuation. For fixed attenuator as a device under test (DUT), a medium value (≤ 60 dB) attenuator is used as the GBA which connected directly between the test ports, then high attenuation of the DUT is measured in two setups as follows. 1) Thru and GBA with normal power level and 2) GBA and DUT with higher power level. This approach removes the need to isolate the GBA, therefore, accurate measurements of high attenuation can be obtained simply over a broad frequency range. For variable or step attenuator as a DUT, one of the attenuation sections of the DUT is applied as the GBA. Detailed analyses and those verification measurements are carried out both for fixed attenuator, as well as for variable attenuator and show good agreement.

key words: Attenuation measurement, mismatch, gauge block attenuator, radio frequency, microwave.

1. Introduction

Measurement capabilities of radio frequency (RF) and microwave (MW) attenuation measurement systems are limited to the linearity or dynamic range of the detectors or receivers used, i.e., the difference between the compression power level and the noise level of the receiver [1]-[7]. To overcome this restriction, a double-step measurement technique using a gauge block attenuator (GBA) was developed [8]-[15]. The GBA, which is repeatable step attenuator, is switched on when the test ports in thru state and switched off when the DUT is inserted into the test port to keep good linearity of the receiver during the measurement. In order to minimize the mismatch effect, the GBA needs to be sufficiently isolated using isolation devices such as isolators and attenuator pads. However, this approach narrows the measurement bandwidth due to the limited frequency response of the isolators or reduces the measurement range due to the insertion loss of the attenuator pads. In [16], a particular technique applicable only to step attenuators consisting of three or four attenuator sections with relatively low individual attenuation values such as 10 dB, 20 dB, 30 dB or 40 dB [17],[18] was proposed based on the cascaded 2-port network and S-parameter theory [19]-[22]. High attenuation is obtained by combining the S parameter measurement results of each section. This technique will correct the mismatch losses that occur

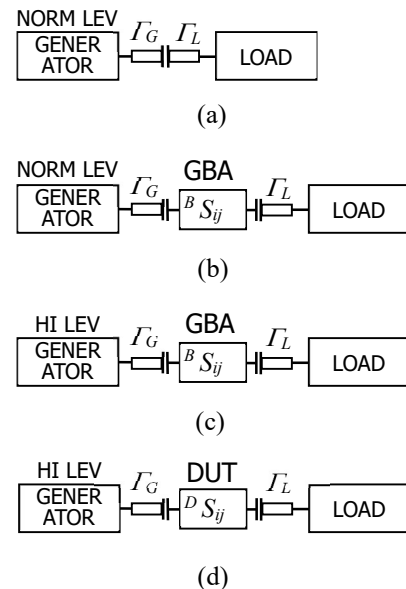


Fig. 1 Schematic outline of double step attenuation measurement technique for a fixed-attenuator. Step-1: (a) Thru connection and (b) GBA in the network with normal input signal. Step-2: (c) GBA and (d) DUT in the network with higher input signal.

between the sections of the step attenuator to be measured. However, it will fail if crosstalk or leakage occurs between the sections.

This paper presents a simple double-step attenuation measurement technique using a non-isolating GBA to facilitate accurate measurements of RF and MW high attenuation, i.e., greater than 60 dB. In contrast to the systems described in the literature, the GBA is inserted into the DUT insertion port directly without isolation devices. For measurement of a high attenuation fixed attenuator, a medium attenuation (≤ 60 dB) fixed attenuator is used as a GBA, and the attenuation of the DUT is measured as follows. In Step-1, attenuation which occurs between its thru connection and the GBA in the line is measured. In Step-2, the power level of the RF generator is increased appropriately and the attenuation which occurs between the GBA and the DUT in the line is measured. The GBA reduces the increased power level, then the receiver will not be overloaded or saturated. The attenuation of the DUT then is obtained by adding up these two-step attenuation measurement results. This approach removes the need to isolate the GBA; however, no mismatch errors will occur in

The author is with National Metrology Institute of Japan (NMIJ), National Institute of Advanced Industrial Science and Technology (AIST), Tsukuba-shi, 305-8563 Japan.

addition to those defined in the attenuation measurement principle [23]-[25]. Therefore, the proposed technique simplifies the structure of the system and allows the accurate measurement of high attenuation to be performed without being limited by the frequency bandwidth of the isolation devices. For attenuation measurement of variable or step attenuators, one of the attenuator sections of the DUT is employed as the GBA [26]. The adequacy of this proposed technique is evaluated by using the S-parameter analyses and verified by carrying out some experimental attenuation measurements.

2. Measurement Technique Analysis

The principle and measurement procedure of the proposed double-step technique has been detailed in the introduction, where by inserting the GBA into the test port, high attenuation is measured in two steps both of which can be performed at good system linearity with low noise effects. In this section the proposed double technique will be investigated with the S-parameter analysis to prove that the obtained results coincide with the definition of attenuation.

2.1 Fixed Attenuator

Fig. 1 is a schematic outline of the double-step attenuation measurement procedure for a fixed-attenuator. A GBA of a medium value of fixed attenuator is introduced into the network in addition to the normal configuration of thru connection and the DUT in the line. This differs from the previous double step techniques in the literature, since the GBA is inserted into the test ports directly without the need of a RF isolator, thus simplifies the structure of the system and removes the bandwidth limits. In Step-1 (Fig.1 (a), (b)) insertion loss which occurs between its thru and the GBA in the line is measured as L_{I1} . Using the signal flow graph and the non-touching loop rule[27]-[29], L_{I1} is expressed in decibels as follows.

$$L_{I1} = 20 \log_{10} \frac{|(1 - {}^B S_{11} \Gamma_G)(1 - {}^B S_{22} \Gamma_L) - {}^B S_{21} {}^B S_{12} \Gamma_G \Gamma_L|}{|{}^B S_{21}| \cdot |1 - \Gamma_G \Gamma_L|} \quad (1)$$

Where, ${}^B S_{ij}$ are the scattering coefficients of the GBA. Γ_G and Γ_L are the source and load reflection coefficients appeared on the test ports, respectively.

In Step-2 (Fig.1 (c) and (d)), the power level of the source is increased appropriately (e.g., 20 dBm) and the insertion loss which occurs between the GBA and the DUT in the line is measured as L_{I2} and is expressed in decibels as follows.

$$L_{I2} = 20 \log_{10} \frac{|{}^D S_{21}| \cdot |(1 - {}^D S_{11} \Gamma_G)(1 - {}^D S_{22} \Gamma_L) - {}^D S_{21} {}^D S_{12} \Gamma_G \Gamma_L|}{|{}^D S_{21}| \cdot |(1 - {}^B S_{11} \Gamma_G)(1 - {}^B S_{22} \Gamma_L) - {}^B S_{21} {}^B S_{12} \Gamma_G \Gamma_L|} \quad (2)$$

Where, ${}^D S_{ij}$ is the scattering coefficients of the DUT. By adding L_{I1} of (1) and L_{I2} of (2), all items related to the

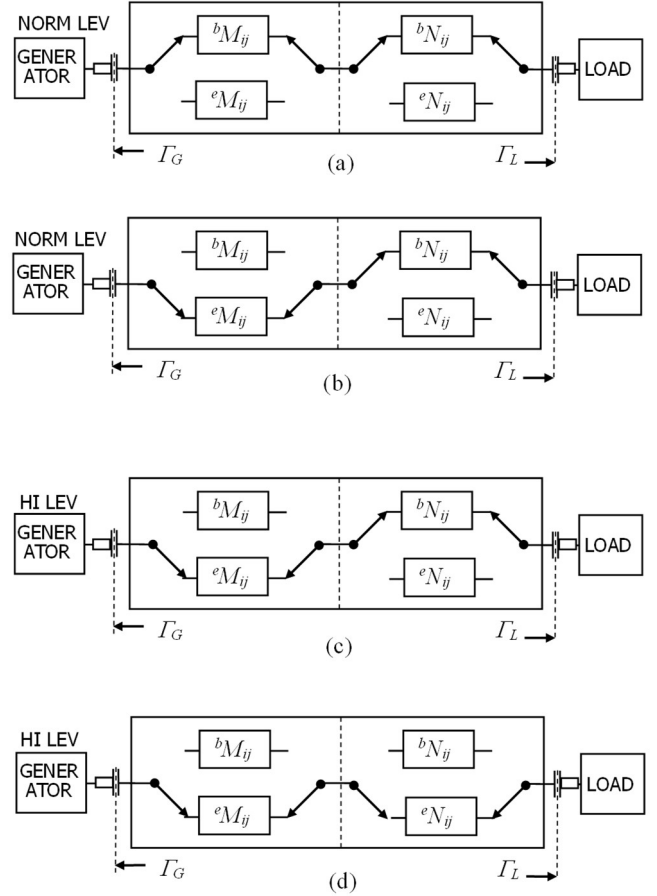


Fig. 2 Schematic outline of double step attenuation measurement technique for a variable attenuator. Step-1: (a) initial setting and (b) GBA setting with normal level input signal. Step-2: (c) GBA setting and (d) final setting with high level output.

GBA vanish, and the following expression is found.

$$L_I = L_{I1} + L_{I2} = 20 \log_{10} \frac{|(1 - {}^D S_{11} \Gamma_G)(1 - {}^D S_{22} \Gamma_L) - {}^D S_{21} {}^D S_{12} \Gamma_G \Gamma_L|}{|{}^D S_{21}| \cdot |1 - \Gamma_G \Gamma_L|} \quad (3)$$

L_I of (3) expresses the insertion loss (dB) of the DUT as defined [23]-[25]. Assuming that Γ_G and Γ_L are matched (Γ_G and $\Gamma_L = 0$), the attenuation, A (dB) of the DUT can be found as follows.

$$A = 20 \log_{10} \frac{1}{|{}^D S_{21}|} \quad (4)$$

Equations (3) and (4) show that the results obtained with the proposed double step technique are identical to the insertion loss and attenuation definitions, respectively, without mismatch errors caused by the GBA [23]-[25].

2.2 Variable Attenuator

Figure 2 shows the circuit model of a variable step attenuator (DUT) composed of two step attenuator sections M and N ,

where ${}^bM_{ij}$ and ${}^bN_{ij}$ are the scattering coefficients of the M and N at the initial settings, while ${}^eM_{ij}$ and ${}^eN_{ij}$ are the scattering coefficients of the M and N set to the final positions, respectively. The model is connected between the measurement ports of the attenuation measurement system. Three nominal attenuations (incremental attenuations) can be set in this model by switching its datum position (${}^bM_{ij}$, ${}^bN_{ij}$) to setting positions, i.e., (${}^eM_{ij}$, ${}^eN_{ij}$), (${}^bM_{ij}$, ${}^eN_{ij}$) and (${}^eM_{ij}$, ${}^eN_{ij}$). The third setting is representative of the step attenuator configuration to produce higher attenuation by combining two attenuator sections or more.

1. Normal Attenuation Measurement Technique

This subsection describes the expressions for the substitution loss and incremental attenuation of the model when is measured by using the normal technique as defined [23]-[25]. This is to facilitate the validation of the results obtained by the proposed double step technique described in the next subsection.

When the step attenuator of the model is switched from its datum position (${}^bM_{ij}$, ${}^bN_{ij}$), as shown in figure 2(a), to final position (${}^eM_{ij}$, ${}^eN_{ij}$) as shown in figure 2(d), the substitution loss that occurs is measured as and is expressed in decibels as follows (see Appendix (A-1), (A-2)).

$$L_s^{MN} = 20 \log_{10} \frac{|{}^bM_{21} {}^bN_{21}|}{|{}^eM_{21} {}^eN_{21}|} + 20 \log_{10} \frac{|1 - {}^eM_{22} {}^eN_{11} + {}^eP\Gamma_G + {}^eQ\Gamma_L + {}^eR\Gamma_G\Gamma_L|}{|1 - {}^bM_{22} {}^bN_{11} + {}^bP\Gamma_G + {}^bQ\Gamma_L + {}^bR\Gamma_G\Gamma_L|} \quad (5)$$

Where,

$${}^{b,e}P = {}^{b,e}M_{11} {}^{b,e}M_{22} {}^{b,e}N_{11} - {}^{b,e}M_{11} - {}^{b,e}M_{21} {}^{b,e}M_{12} {}^{b,e}N_{11} \quad (6)$$

$${}^{b,e}Q = {}^{b,e}M_{22} {}^{b,e}N_{11} {}^{b,e}N_{22} - {}^{b,e}N_{22} - {}^{b,e}M_{22} {}^{b,e}N_{21} {}^{b,e}N_{12} \quad (7)$$

$${}^{b,e}R = {}^{b,e}M_{11} {}^{b,e}N_{22} - {}^{b,e}M_{21} {}^{b,e}M_{12} {}^{b,e}N_{21} {}^{b,e}N_{12} - {}^{b,e}M_{11} {}^{b,e}M_{22} {}^{b,e}N_{11} {}^{b,e}N_{22} \quad (8)$$

The incremental attenuation, A_{inc}^{MN} (dB), of the DUT then can be found by (5) by setting both Γ_G and Γ_L equal to zero as follows [23]-[25].

$$A_{inc}^{MN} = 20 \log_{10} \frac{|{}^bM_{21} {}^bN_{21}|}{|{}^eM_{21} {}^eN_{21}|} + 20 \log_{10} \frac{|1 - {}^eM_{22} {}^eN_{11}|}{|1 - {}^bM_{22} {}^bN_{11}|} \quad (9)$$

It is found that the incremental attenuation of the model consists of the attenuation of each attenuator section, shown by the first term on the right side of (9), plus the mismatch losses that occur between the attenuator sections, shown by the second term on the right side of (9).

2. Double Step Attenuation Measurement Technique

In this double step attenuation measurement technique, the front section attenuator of the DUT is acted as the GBA. In Step-1, substitution loss of the DUT is measured as when its datum position of (${}^bM_{ij}$, ${}^bN_{ij}$) (Fig. 2(a)) is switched to

the GBA attenuation position of (${}^eM_{ij}$, ${}^bN_{ij}$) (Fig. 2(b)). Similar to (5), L_s^{MNb} is expressed in decibels as follows.

$$L_s^{MNb} = 20 \log_{10} \frac{|{}^bM_{21}|}{|{}^eM_{21}|} + 20 \log_{10} \frac{|1 - {}^eM_{22} {}^bN_{11} + U\Gamma_G + V\Gamma_L + W\Gamma_G\Gamma_L|}{|1 - {}^bM_{22} {}^bN_{11} + {}^bP\Gamma_G + {}^bQ\Gamma_L + {}^bR\Gamma_G\Gamma_L|} \quad (10)$$

Where,

$$U = {}^eM_{11} {}^eM_{22} {}^bN_{11} - {}^eM_{11} - {}^eM_{21} {}^eM_{12} {}^bN_{11} \quad (11)$$

$$V = {}^eM_{22} {}^bN_{11} {}^bN_{22} - {}^bN_{22} - {}^eM_{22} {}^bN_{21} {}^bN_{12} \quad (12)$$

$$W = {}^eM_{11} {}^bN_{22} - {}^eM_{21} {}^eM_{12} {}^bN_{21} {}^bN_{12} - {}^eM_{11} {}^eM_{22} {}^bN_{11} {}^bN_{22} \quad (13)$$

In Step-2, the power level of the source is increased appropriately and the substitution loss of the DUT is measured as L_s^{MNe} when its datum position of (${}^eM_{ij}$, ${}^bN_{ij}$) (Fig. 2(c)) is switched to (${}^eM_{ij}$, ${}^eN_{ij}$) (Fig. 2(d)). L_s^{MNe} is expressed in decibels as

$$L_s^{MNe} = 20 \log_{10} \frac{|{}^bN_{21}|}{|{}^eN_{21}|} + 20 \log_{10} \frac{|1 - {}^eM_{22} {}^eN_{11} + {}^eP\Gamma_G + {}^eQ\Gamma_L + {}^eR\Gamma_G\Gamma_L|}{|1 - {}^eM_{22} {}^bN_{11} + U\Gamma_G + V\Gamma_L + W\Gamma_G\Gamma_L|} \quad (14)$$

By adding L_s^{MNb} of (10) and L_s^{MNe} of (14), the following expression is found.

$$L_s^{MNb} + L_s^{MNe} = 20 \log_{10} \frac{|{}^bM_{21} {}^bN_{21}|}{|{}^eM_{21} {}^eN_{21}|} + 20 \log_{10} \frac{|1 - {}^eM_{22} {}^eN_{11} + {}^eP\Gamma_G + {}^eQ\Gamma_L + {}^eR\Gamma_G\Gamma_L|}{|1 - {}^bM_{22} {}^bN_{11} + {}^bP\Gamma_G + {}^bQ\Gamma_L + {}^bR\Gamma_G\Gamma_L|} \quad (15)$$

Equation (15) expresses the substitution loss of the DUT, identical to that obtained using the normal technique as in (5). This proves the validity of the proposed double step technique for measurements of high attenuation variable attenuators. By setting both Γ_G and Γ_L of (15) equal to zero, incremental attenuation of the DUT is immediately obtained as in (9).

3. Measurement Result

All measurement results described in this section were obtained using the general-purpose RF receiver system which works on the principle of intermediate frequency (IF=30 MHz) substitution technique [30][31]. The N9010B signal analyzer was used as the sensitive level detector with the following settings. Central Frequency: 30 MHz. Frequency Span: 0 Hz. Resolution and Video Bandwidth: 1 kHz. Averaging: 100 times. The system was tested has a dynamic range of over 60 dB with an accuracy of better than 0.001 dB, and 80 dB with an accuracy of 0.01 dB without

nonlinearity correction. The measurement room conditions were controlled at room temperature $23^{\circ}\text{C} \pm 2^{\circ}\text{C}$ and relative humidity $40\% \pm 20\%$.

To verify the accuracy of the proposed double step technique, measurements on low value attenuations both of fixed and variable attenuators were carried out and the results were compared to the one of the normal (direct) measurement technique.

For attenuation values equal to or less than 30 dB, it is predicted that the system uncertainties caused by the nonlinearity is negligible small.

Table 1 shows the results for a nominal value of 30 dB of fixed attenuator as a DUT, measured at simultaneously frequency from 1 GHz to 17 GHz, in 4 GHz intervals. A nominal 10 dB fixed attenuator was used as a GBA. The

Table 1 Measurement results of small attenuation of a particular fixed attenuator.

DUT: 30 dB, GBA: 10 dB					
Freq	Proposed Technique			Normal	Difference
	Step-1	Step-2	Result	Technique	
	A	B	R=(A+B)	N	R-N
[GHz]	[dB]	[dB]	[dB]	[dB]	[dB]
1	9.919	19.776	29.695	29.695	0.000
5	9.986	19.783	29.769	29.771	-0.002
9	10.020	19.767	29.787	29.786	0.001
13	10.094	19.772	29.866	29.866	0.000
17	10.012	19.753	29.765	29.766	-0.001

Table 2 Measurement results of small attenuation of a particular step attenuator at 12 GHz.

DUT		GBA Setting		Proposed Technique			Normal	Difference
Nom. Value	Switch	Nom. Value	Switch	Step-1	Step-2	Result	Technique	
[dB]		[dB]		A	B	R=(A+B)	N	R-N
[dB]		[dB]		[dB]	[dB]	[dB]	[dB]	[dB]
3	1, 2	1	1	1.003	2.031	3.034	3.034	0.000
5	1, 3	1	1	1.003	3.968	4.971	4.972	-0.001
6	2, 3	2	2	2.045	3.973	6.018	6.017	0.001
8	3, 4	4	3	3.954	3.933	7.887	7.887	0.000

proposed technique measured the attenuations of the DUT in two steps. The first step was attenuation measurements of the thru connection and the GBA in the network settings. The second step was of the GBA and the DUT in the network settings. The results are shown in the second and third columns of the table, respectively. The attenuations of the DUT then are obtained by adding these two step results as shown in the fourth column of the table. For comparison, attenuation measurements using the normal (direct) measurement technique were also performed, and the results are shown in the fifth column of the table. It is found that the results from the proposed technique agree well (with a maximum difference ± 0.002 dB) with the normal technique results.

Similar measurements are also made for a given step attenuator, which consists of 4 attenuator sections: 1-dB (switch 1), 2-dB (switch 2), 4-dB (switch 3) and 4-dB (switch 4), which can be set from 1 dB to 11 dB in 1 dB steps. Table 2 shows the results for the nominal values of 3, 5, 6, 8 dBs, measured at frequency of 12 GHz. Basically, any attenuator section can be used as the GBA, but in this experiment, the front section was applied for 3, 5 and 6 dB measurements and the back section for 8 dB measurements. Good agreements were also obtained (with a maximum difference ± 0.001 dB) between the results by the proposed technique and by the normal technique.

The effectiveness of this technique was investigated by measuring high attenuation values of both fixed and step attenuator. Table 3 shows the results for a nominal value of 80 dB of fixed attenuator as a DUT, measured at

Table 3 Measurement results of high attenuation of a particular fixed attenuator.

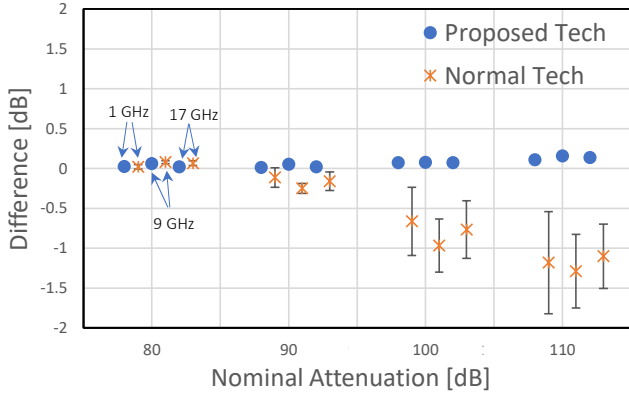
DUT: 80 dB, GBA: 50 dB					
Freq	Step-1		Step-2		Result
	Meas	Std Dev	Meas	Std Dev	
	A		B		R=(A+B)
[GHz]	[dB]	[dB]	[dB]	[dB]	[dB]
9	50.346	0.002	30.294	0.005	80.640
11	50.246	0.001	30.406	0.008	80.652
13	50.407	0.001	30.407	0.005	80.814
15	50.635	0.002	30.276	0.010	80.911
17	50.384	0.001	30.018	0.010	80.402

simultaneously frequency from 9 GHz to 17 GHz, in 2 GHz intervals. A nominal 50 dB fixed attenuator was used as a GBA. Table 4 shows the results for the nominal values of 60, 80, 100 dBs of a step attenuator as a DUT, measured at frequency of 12 GHz. This attenuator consists of 4 attenuator sections: 10-dB (switch 1), 20-dB (switch 2), 40-dB (switch 3) and 40-dB (switch 4). For comparison, attenuation measurements using the previous GBA technique [12] were also performed and the results are shown in the eighth column of the table. Both results exhibited good agreement.

Fig.3 shows the improvement effects of the proposed technique in high attenuation measurements compared to the normal technique. A step attenuator with nominal values of 80 dB, 90 dB, 100 dB and 110 dB indicated by the horizontal

Table 4 Measurement results of high attenuation of a particular step attenuator at 12 GHz.

DUT		GBA Setting		Proposed Technique			Prev Gauge Block Tech	Difference
Nom Value	Switch	Nom Value	Switch	Step-1	Step-2	Result	N	
[dB]		[dB]		[dB]	[dB]	[dB]	[dB]	[dB]
60	2, 3	40	3	40.331	20.053	60.384	60.383	0.001
80	3, 4	40	3	40.331	40.347	80.678	80.679	-0.001
100	2, 3, 4	60	2,3	60.384	40.351	100.735	100.738	-0.003


Fig. 3 Improvement effects of the proposed technique by comparing with the normal technique.

axis were measured at frequencies of 1 GHz, 9 GHz, and 17 GHz. The results obtained by the normal technique are indicated by asterisk, and the results obtained by the proposed technique are indicated by filled circles. The measurement results are normalized to each nominal value and displayed as a difference in dB as on the vertical axis. Vertical error bars indicate the standard deviation with a repetition error number of 10. It is found that the results obtained by the proposed technique are almost the same and do not differ by more than 0.3 dB from the nominal value. However, the results obtained with normal technique are highly different at high nominal values and also have large standard deviations.

4. Conclusion

A double step technique for accurate measurement of high attenuation of RF attenuators was improved by introducing a gauge block attenuator inserted into the test ports directly in additions to the normal measurement procedure. This technique simplified the structure of the system by removing the isolators from the GBA without affecting additional mismatch errors and allowed the accurate measurement of high attenuation RF attenuators to be done in a wide frequency range. The adequacy of this proposed technique was evaluated by using the S-parameter analyses and verified by carrying out some experimental measurements over various values of attenuations and frequencies. Comparisons with measurements obtained using the normal technique for low attenuation and the previous GBA

technique for high attenuation showed good agreement.

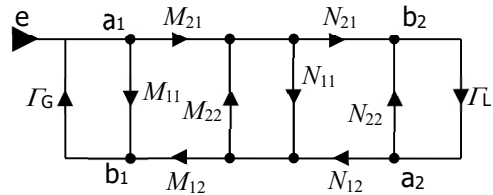
Appendix

Fig. A1 is the signal flow graph for the network configuration given in Fig. 2(a). Using the Mason non-touching loop rule [27]-[29], the ratio b_2/e of the complex wave amplitude at e to that at an independent point b_2 is expressed as follows.

$$\begin{aligned}
 b_2/e = & M_{21}N_{21}/\{1 - (\Gamma_G M_{11} + M_{22}N_{11} + N_{22}\Gamma_L \\
 & + \Gamma_G M_{21}N_{11}M_{12} + M_{22}N_{21}\Gamma_L N_{12} \\
 & + \Gamma_G M_{21}N_{21}\Gamma_L N_{12}M_{12}) \\
 & + (\Gamma_G M_{11}M_{22}N_{11} + \Gamma_G M_{11}N_{22}\Gamma_L + M_{22}N_{11}N_{22}\Gamma_L) \\
 & - (\Gamma_G M_{11}M_{22}N_{11}N_{22}\Gamma_L)\} \quad (A.1)
 \end{aligned}$$

Rearranging the denominator, (A.1) becomes as follows.

$$\begin{aligned}
 b_2/e = & M_{21}N_{21}/\{1 - M_{22}N_{11} \\
 & + (M_{11}M_{22}N_{11} - M_{11} - M_{21}M_{12}N_{11})\Gamma_G \\
 & + (M_{22}N_{11}N_{22} - N_{22} - M_{22}N_{21}N_{12})\Gamma_L \\
 & + (M_{11}N_{22} - M_{21}M_{12}N_{21}N_{12} - M_{11}M_{22}N_{11}N_{22})\Gamma_G\Gamma_L\} \quad (A.2)
 \end{aligned}$$


Fig. A1 Signal flow graph of cascaded two port devices M and N .

References

- [1] R.K. McDowel, "High dynamic range receiver parameters," Tech-Notes, Vol. 7 No. 2, March/April 1980.
- [2] R.E. Watson, "Receiver dynamic range: part 1," Tech-Notes, Vol. 14 No. 1 January/February 1987.
- [3] D. K. Rytting, "Network analyzer accuracy overview," 58th ARFTG Conference Digest, San Diego, CA, USA, 2001, pp. 1-13, doi: 10.1109/ARFTG.2001.327486.
- [4] Y.Ding, M. Trinkle, "Dynamic range considerations for wideband Zero-IF receivers," 4th IEEE Conference on Industrial Electronics and Applications, Xi'an, China, May 25-27, 2009, 1976-1981.
- [5] K. Wong, "VNA receiver dynamic accuracy specifications and uncertainties - A top level overview", White Paper, June 25, 2010

- [6] H. De Los Santos, C. Sturm, J. Pontes, "Sensitivity and dynamic range," in *Radio Systems Engineering*, pp 137–154. Springer, Cham, 2015. doi: 10.1007/978-3-319-07326-2_6.
- [7] J. Mortensen, R. Sturdivant, M. Wickert, "Dynamic range definitions and measurement applied to radar digital receiver exciter (DREX)," in *Digest 97th ARFTG Microwave Measurement Conference (ARFTG)*, Atlanta, GA, USA, March 2021.
- [8] F.L. Warner et al., "Recent improvements to the UK national microwave attenuation standards," *IEEE Trans. Instrum. Meas.*, vol.32, no.1, pp. 33-37, March 1983.
- [9] F.L. Warner and P. Herman, "Very precise measurement of attenuation over a 90 dB using voltage ratio plus gauge block technique," *IEE Colloquium, Dig. No. 1983/53*, pp.17/1-17/7, May 1983.
- [10] D. Stumpe, "Recent developments in the PTB RF standard attenuation measuring equipment" *IEEE Trans. Instrum. Meas.*, vol.40, pp. 652-654, Jun 1991.
- [11] G.J. Kilby, et al., "The accurate measurement of high attenuation at radio frequency," *IEEE Trans. Instrum. Meas.*, vol.44, pp. 308-311, April 1995.
- [12] A. Widarta, et al., "Japan National Standard of Attenuation in the Frequency Range of 10 MHz to 18 GHz", in *Digest CPEM 2004*, London (UK), June 2004, pp.103-104.
- [13] Outline of RF Attenuation Calibration, Japan Quality Assurance Organization, E314379, 1997 (in Japanese).
- [14] T. Wu, et al., "A Dual Channel AF Substitution Microwave Attenuation Measurement System for Precision Attenuator Calibration," *Proc. of NCSLI 2007*, Jul 2007.
- [15] T. Wu, S.W. Chua, "Broadband microwave attenuation measurement standard in the frequency range from 10 MHz to 26.5 GHz," *Proc. of IEEE I2MTC 2009*, Singapore, May 2009
- [16] S. Zhang, "High attenuation measurement of step attenuators," *Cal Lab Magazine*, pp.30-35, April 2011.
- [17] Keysight Technologies, *RF & Microwave Test Accessories – Product Catalog*, Chapt.5, pp.40-47. [Online] Available: <https://connectp.keysight.com/AMORFuWTestAccessoryCatalog>
- [18] Anritsu, *Precision RF & Microwave Components – Product Catalog*, pp. 40-41. [Online] Available: <https://www.rfmw.com/data/anritsu%20product%20catalog1.pdf>
- [19] Hewlett-Packard Co., *Application Note 95-1, S-Parameter Techniques*.
- [20] M.M. Radmanesh, *Radio Frequency and Microwave Electronics Illustrated*, Prentice Hall, Hoboken, NJ, 2001.
- [21] Agilent Technologies Co., *Application Note 5989-5765EN, Part 3: the ABCs of De-Embedding*.
- [22] Agilent Technologies Co., *Application Note 1364-1, DeEmbedding and Embedding S-Parameter Networks Using a Vector Network Analyzer*.
- [23] R. W. Beatty, "Microwave Attenuation Measurements and Standards," *Nat. Bur. Stand. Monograph*, vol. 97, 1967.
- [24] F. L. Warner, *Microwave Attenuation Measurement*, Ch. 2, Peter Peregrinus Ltd, London, U.K., 1977.
- [25] R. Collier, D. Skinner, *Microwave Measurements 3rd ed.* The Institution of Engineering and Technology, Ch. 5, London, UK, 2007.
- [26] A. Widarta, "Double step attenuation measurement technique for high attenuation of variable attenuators", in *Digest CPEM 2012*, Washington DC, July 2012, pp.30-31.
- [27] S.J. Mason, "Feedback theory -Some properties of signal flow graphs," *Proceedings of the IRE*, vol. 41, no. 9, Appx. 2, Sept. 1953.
- [28] S.J. Mason and H.J. Zimmermann, *Electronic circuits, signals, and systems*, John Wiley and Sons, Inc., 1960.
- [29] F. L. Warner, *Microwave Attenuation Measurement*, IEE Monograph Series 19, pp. 273-277, Peter Peregrinus Ltd.1977.
- [30] A. Widarta, "Simple and accurate radio frequency attenuation measurements using general-purpose receiver," in *Proceedings ICEE 2008*, Okinawa, Japan, July 6-10, 2008, O-063.
- [31] A. Widarta, " Working standard for RF attenuation and phase-shift calibrations," in *Digest CPEM 2022*, Wellington, (NZ), Dec.2022.



Anton Widarta was born in Magelang, Indonesia. He received the Dr. Eng. degree from Nihon University, Tokyo, Japan, in 1996. His doctoral work focused on accurate analyses of the electromagnetic field problems in waveguide junctions and discontinuities. He is currently a Senior Research Scientist with the Research Institute for Physical Measurement, National Metrology Institute of Japan (NMIJ), National Institute of Advanced Industrial Science and Technology (AIST), Tsukuba, Japan. He is a lecturer with the College of Engineering, Nihon University. He developed a broadband precision RF/microwave attenuation and phase-shift measurement system to replace the former Japan national standard of attenuation. He also prepared a technical manual for the system under the NMIJ quality system for primary standards and serves as a Deputy Technical Manager. His current research interests include precision high frequency electromagnetic measurement technologies for standards and applications related to energy efficiency. Dr. Widarta is the Co-Chair of the Focus Group on Energy Efficiency of the Asia-Pacific Metrology Programme (APMP).